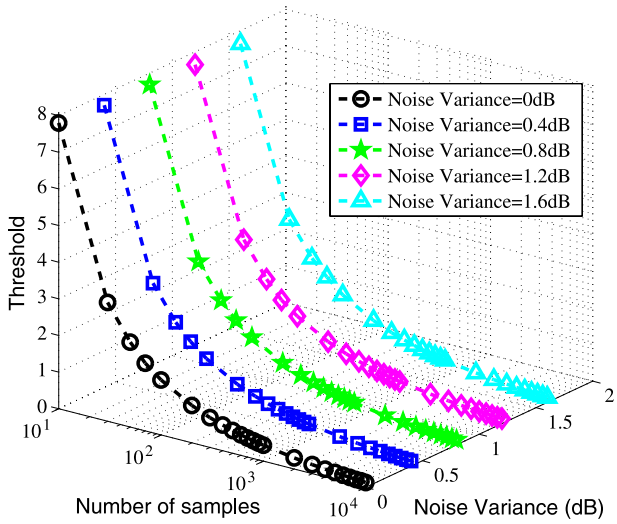

Fig. 6. Three-dimensional plot of the threshold changing with the number of samples and the noise variance: $M = 4$ and $P_{\rm fa} = 0.1$.

AoA information. We also derived the theoretical probability of false alarm and detection threshold. Simulations have been carried out to verify efficiency of the proposed method.

REFERENCES

[1] E. Axell, G. Leus, E. G. Larsson, and H. V. Poor, "Spectrum sensing for cognitive radio: State-of-the-art and recent advances," *IEEE Signal Process. Mag.*, vol. 29, no. 3, pp. 101–116, May 2012.

[2] F. F. Digham, M. S. Alouini, and M. K. Simon, "On the energy detection of unknown signals over fading channels," *IEEE Trans. Commun.*, vol. 55, no. 1, pp. 21–24, Jan. 2007.

[3] Y. Zeng and Y. Liang, "Eigenvalue-based spectrum sensing algorithms for cognitive radio," *IEEE Trans. Commun.*, vol. 57, no. 6, pp. 1784–1793, Jun. 2009.

[4] R. Zhang, T. J. Lim, Y. Liang, and Y. Zeng, "Multi-antenna based spectrum sensing for cognitive radios: A GLRT approach," *IEEE Trans. Commun.*, vol. 58, no. 1, pp. 84–88, Jan. 2010.

[5] Y. Zeng and Y. Liang, "Covariance based signal detections for cognitive radio," in *Proc. IEEE DySPAN*, Dublin, Ireland, Apr. 2007, pp. 202–207.

[6] G. Zhao *et al.*, "Spatial spectrum holes for cognitive radio with relay-assisted directional transmission," *IEEE Trans. Wireless Commun.*, vol. 8, no. 10, pp. 5270–5279, Oct. 2009.

[7] J. Xie, Z. Fu, and H. Xian, "Spectrum sensing based on estimation of direction of arrival," in *Proc. Int. Conf. Comput. Problem-Solving*, Li Jiang, China, Dec. 2010, pp. 39–42.

[8] C. Jiang *et al.*, "Cognitive radio networks with asynchronous spectrum sensing and access," *IEEE Netw.*, vol. 29, no. 3, pp. 88–95, May 2015.

[9] T. S. Dhope and D. Simunic, "On the performance of AoA estimation algorithms in cognitive radio networks," in *Proc. IEEE ICCICT*, Mumbai, India, Oct. 19/20, 2012, pp. 1–5.

[10] C. Liu, M. Li, and M. Jin, "Blind energy based detection for spatial spectrum sensing," *IEEE Wireless Commun. Lett.*, vol. 4, no. 1, pp. 98–101, Feb. 2015.

[11] C. Jiang, Y. Chen, K. J. R. Liu, and Y. Ren,"Renewal-theoretical dynamic spectrum access in cognitive radio network with unknown primary behavior," *IEEE J. Sel. Areas Commun.*, vol. 31, no. 3, pp. 406–416, Mar. 2013.

[12] C. Jiang *et al.*, "DYWAMIT: Asynchronous wideband dynamic spectrum sensing and access system," *IEEE Syst. J.*, May 2013, [Early Access].

[13] C. Jiang, Y. Chen, Y. Gao, and K. J. R. Liu, "Joint spectrum sensing and access evolutionary game in cognitive radio networks," *IEEE Trans. Wireless Commun.*, vol. 12, no. 5, pp. 2470–2483, May 2013.

[14] T. Do and B. L. Mark, "Joint spatial–temporal spectrum sensing for cognitive radio networks," *IEEE Trans. Veh. Technol.*, vol. 59, no. 7, pp. 3480–3490, Sep. 2010.

[15] Q. Wu, G. Ding, J. Wang, and Y. Yao, "Spatial–temporal opportunity detection for spectrum-heterogeneous cognitive radio networks: Two-dimensional sensing," *IEEE Trans. Wireless Commun.*, vol. 12, no. 2, pp. 516–526, Feb. 2013.

[16] A. W. Min, X. Zhang, and K. G. Shin, "Spatio-temporal fusion for small-scale primary detection in cognitive radio networks," in *Proc. IEEE INFOCOM*, San Diego, CA, USA, Mar. 2010, pp. 1–5.

[17] M. S. Bartlett, *An Introduction to Stochastic Processes: With Special Reference to Methods and Applications*. Cambridge, U.K.: Cambridge Univ. Press, 1961.

[18] A. Sahai and D. Cabric, "Tutorial: Spectrum sensing fundamental limits and practical challenges," in *Proc. IEEE DySpan Conf.*, Baltimore, MD, USA, Nov. 2005, pp. 1–90.

[19] H. Yin, D. Gesbert, M. Filippou, and Y. Liu, "A coordinated approach to channel estimation in large-scale multiple-antenna systems," *IEEE J. Sel. Areas Commun.*, vol. 31, no. 2, pp. 264–273, Feb. 2013.

[20] B. D. Van Veen *et al.*, "Beamforming: A versatile approach to spatial filtering," *IEEE ASSP Mag.*, vol. 5, no. 2, pp. 4–24, Apr. 1988.

[21] L. Mirsky, "A trace inequality of John von Neumann," *Monatshefte für Mathematik*, vol. 79, no. 4, pp. 303–306, Dec. 1975.

Nonorthogonal Multiple Access in Large-Scale Underlay Cognitive Radio Networks

Yuanwei Liu, *Student Member, IEEE*,
Zhiguo Ding, *Senior Member, IEEE*,
Maged Elkashlan, *Member, IEEE*, and Jinhong Yuan, *Fellow, IEEE*

***Abstract*—In this paper, nonorthogonal multiple access (NOMA) is applied to large-scale underlay cognitive radio (CR) networks with randomly deployed users. To characterize the performance of the considered network, new closed-form expressions of the outage probability are derived using stochastic geometry. More importantly, by carrying out the diversity analysis, new insights are obtained under the two scenarios with different power constraints: 1) fixed transmit power of the primary transmitters (PTs); and 2) transmit power of the PTs being proportional to that of the secondary base station. For the first scenario, a diversity order of m is experienced at the mth-ordered NOMA user. For the second scenario, there is an asymptotic error floor for the outage probability. Simulation results are provided to verify the accuracy of the derived results. A pivotal conclusion is reached that by carefully designing target data rates and power allocation coefficients of users, NOMA can outperform conventional orthogonal multiple access in underlay CR networks.**

***Index Terms*—Cognitive radio (CR), large-scale network, nonorthogonal multiple access (NOMA), stochastic geometry.**

I. INTRODUCTION

Spectrum efficiency is of significant importance and becomes one of the main design targets for future fifth-generation networks. Nonorthogonal multiple access (NOMA) has received considerable attention because of its potential to achieve superior spectral efficiency [1]. Particularly, different from conventional multiple-access (MA)

Manuscript received May 9, 2015; revised December 12, 2015 and January 16, 2016; accepted January 20, 2016. Date of publication February 3, 2016; date of current version December 14, 2016. The review of this paper was coordinated by Dr. S. Tomasin.

Y. Liu and M. Elkashlan are with Queen Mary University of London, London E1 4NS, U.K. (e-mail: yuanwei.liu@qmul.ac.uk; maged.elkashlan@qmul.ac.uk).

Z. Ding is with Lancaster University, Lancaster LA1 4YW, U.K. (e-mail: z.ding@lancaster.ac.uk).

J. Yuan is with the University of New South Wales, Sydney, NSW 2052, Australia (e-mail: j.yuan@unsw.edu.au).

Digital Object Identifier 10.1109/TVT.2016.2524694

techniques, NOMA uses the power domain to serve multiple users at different power levels to use the spectrum more efficiently. A downlink NOMA and an uplink NOMA are considered in [2] and [3], respectively. The application of multiple-input multiple-output (MIMO) techniques to NOMA has been considered in [4] by using zero-forcing detection matrices. Sun *et al.* in [5] investigated an ergodic capacity maximization problem for MIMO NOMA systems.

Another approach to improve spectrum efficiency is the paradigm of underlay cognitive radio (CR) networks, which was proposed in [6] and has rekindled increasing interest in using the spectrum more efficiently. The key idea of underlay CR networks is that each secondary user (SU) is allowed to access the spectrum of the primary users (PUs) as long as the SU meets a certain interference threshold in the primary network (PN). In [7], an underlay CR network taking into account the spatial distribution of the SU relays and PUs was considered, and its performance was evaluated by using stochastic geometry tools. In [8], a new CR-inspired NOMA scheme has been proposed, and the impact of user pairing has been examined, by focusing on a simple scenario with only one primary transmitter (PT).

By introducing the aforementioned two concepts, it is natural to consider the application of NOMA in underlay CR networks using additional power control at the secondary base station (BS) to improve the spectral efficiency. Stochastic geometry is used to model a large-scale CR network with a large number of randomly deployed PTs and primary receivers (PRs). We consider a practical system design as follows: 1) All the SUs, PTs, and PRs are randomly deployed based on the considered stochastic geometry model; 2) each SU suffers interference from other NOMA SUs as well as the PTs; and 3) the secondary BS must satisfy a predefined power constraint threshold to avoid interference at the PRs. New closed-form expressions of the outage probability of the NOMA users are derived to evaluate the performance of the considered CR NOMA network. Moreover, considering two different power constraints at the PTs, diversity order[1] analysis is carried out with providing important insights: 1) When the transmit power of the PTs is fixed, the mth user among all ordered NOMA user experiences a diversity order of m; and 2) when the transmit power of the PTs is proportional to that of the secondary BS, an asymptotic error floor exists for the outage probability.

II. Network Model

We consider a large-scale underlay spectrum sharing scenario consisting of the PN and the secondary network (SN). In the SN, we consider that a secondary BS is located at the origin of a disc, which is denoted by $\mathcal{D}$ with radius R_D as its coverage. The M randomly deployed SUs are uniformly distributed within the disc, which is the user zone for NOMA. The secondary BS communicates with all SUs within the disc by applying the NOMA transmission protocol. It is worth pointing out that the power of the secondary transmitter is constrained to limit the interference at the PRs. In the PN, we consider a random number of PTs and PRs distributed in an infinite two-dimensional plane. The spatial topology of all the PTs and PRs is modeled using homogeneous Poisson point processes (PPPs), which are denoted by Φ_b and Φ_ℓ with density λ_b and λ_ℓ, respectively. All channels are assumed to be quasi-static Rayleigh fading where the channel coefficients are constant for each transmission block but vary independently between different blocks.

[1]Diversity order is defined as the slope for the outage provability curve decreasing with the signal-to-noise ratio (SNR). It measures the number of independent fading paths over which the data are received. In NOMA networks, since users' channels are ordered and successive interference cancelation (SIC) is applied at each receiver, it is of importance to investigate the diversity order.

According to underlay CR, the transmit power P_t at the secondary BS is constrained as follows:

$$P_t = \min\left\{\frac{I_p}{\max\limits_{\ell\in\Phi_\ell}|g_\ell|^2}, P_s\right\} \tag{1}$$

where I_p is the maximum permissible interference power at the PRs, P_s is the maximum transmission power at the secondary BS, and $|g_\ell|^2 = |\hat{g}_\ell|^2 L(d_\ell)$ is the overall channel gain from the secondary BS to PRs ℓ. Here, $\hat{g}_\ell$ is small-scale fading with $\hat{g}_\ell \sim \mathcal{CN}(0,1)$, $L(d_\ell) = 1/(1+d_\ell^\alpha)$ is the large-scale path loss, d_ℓ is the distance between the secondary BS and the PRs, and α is the path-loss exponent. A bounded path-loss model is used to ensure that the path loss is always larger than 1 even for small distances [2], [9].

According to NOMA, the BS sends a combination of messages to all NOMA users, and the observation at the mth SU is given by

$$y_m = h_m \sum_{n=1}^{M} \sqrt{a_n P_t} x_n + n_m \tag{2}$$

where n_m is the additive white Gaussian noise at the mth user with variance σ^2, a_n is the power allocation coefficient for the nth SU with $\sum_{n=1}^{M} a_n = 1$, x_n is the information for the nth user, and h_m is the channel coefficient between the mth user and the secondary BS.

For the SUs, they also observe the interferences of the randomly deployed PTs in the PN. Usually, when the PTs are close to the secondary NOMA users, they will cause significant interference. To overcome this issue, we introduce an interference guard zone D_0 to each secondary NOMA user with a radius of d_0, which means that there is no interference from PTs allowed inside this zone [10]. We assume $d_0 \geq 1$ in this paper. The interference links from the PTs to the SUs are dominated by the path loss and given by $I_B = \sum_{b\in\Phi_b} L(d_b)$, where $L(d_b) = 1/(1+d_b^\alpha)$ is the large-scale path loss, and d_b is the distance from the PTs to the SUs.

Without loss of generality, all the channels of SUs are assumed to follow the order as $|h_1|^2 \leq |h_2|^2 \leq \cdots \leq |h_M|^2$. The power allocation coefficients are assumed to follow the order as $a_1 \geq a_2 \geq \cdots \geq a_M$. According to the NOMA principle, SIC is carried out at the receivers [11]. It is assumed that $1 \leq j \leq m < i$. In this case, the mth user can decode the message of the jth user and treats the message for the ith user as interference. Specifically, the mth user first decodes the messages of all the $(m-1)$ users and then successively subtracts these messages to obtain its own information. Therefore, the received signal-to-interference-plus-noise ratio (SINR) for the mth user to decode the information of the jth user is given by

$$\gamma_{m,j} = \frac{|h_m|^2 \gamma_t a_j}{|h_m|^2 \gamma_t \sum\limits_{i=j+1}^{M} a_i + \rho_b I_B + 1} \tag{3}$$

where $\gamma_t = \min\{(\rho_p/\max_{\ell\in\Phi_\ell}|g_\ell|^2), \rho_s\}$, $\rho_p = I_p/\sigma^2, \rho_s = P_s/\sigma^2, \rho_b = P_B/\sigma^2$, and P_B is the transmit power of the PTs, $|h_m|^2$ is the overall ordered channel gain from the secondary BS to the mth SU. For the case $m = j$, it indicates that the mth user decodes the message of itself. Note that the SINR for the Mth SU is $\gamma_{M,M} = (|h_M|^2 \gamma_t a_M/(\rho_b I_B + 1))$.

III. Outage Probability

Here, we provide the exact analysis of the considered networks in terms of outage probability. In NOMA, an outage occurs if the mth user cannot detect any of the jth user's messages, where $j \leq m$ due to SIC. Denote $X_m = |h_m|^2 \gamma_t/(\rho_b I_B + 1)$. Based on (3), the cumulative distribution function (cdf) of X_m is given by

$$F_{X_m}(\varepsilon) = \Pr\left\{\frac{|h_m|^2\gamma_t}{\rho_b I_B + 1} < \varepsilon\right\}. \tag{4}$$

We denote $\varepsilon_j = \tau_j/(a_j - \tau_j \sum_{i=j+1}^{M} a_i)$ for $j < M$, $\tau_j = 2^{R_j} - 1$, R_j is the target data rate for the jth user, $\varepsilon_M = \tau_M/a_M$, and $\varepsilon_m^{\max} = \max\{\varepsilon_1, \varepsilon_2, \ldots, \varepsilon_m\}$. The outage probability at the mth user can be expressed as follows:

$$P_m = \Pr\left\{X_m < \varepsilon_m^{\max}\right\} = F_{X_m}\left(\varepsilon_m^{\max}\right) \tag{5}$$

where the condition $a_j - \tau_j \sum_{i=j+1}^{M} a_i > 0$ should be satisfied due to applying NOMA; otherwise, the outage probability will always be 1 [2].

We need calculate the cdf of X_m conditioned on I_B and γ_t. Rewrite (4) as follows:

$$F_{X_m|I_B,\gamma_t}(\varepsilon) = F_{|h_m|^2}\left(\frac{(\rho_b I_B + 1)\varepsilon}{\gamma_t}\right) \tag{6}$$

where $F_{|h_m|^2}$ is the cdf of h_m. Based on order statistics [12] and applying binomial expansion, the cdf of the ordered channels has a relationship with the unordered channels as follows:

$$F_{|h_m|^2}(y) = \psi_m \sum_{p=0}^{M-m} \binom{M-m}{p} \frac{(-1)^p}{m+p} \left(F_{|\tilde{h}|^2}(y)\right)^{m+p} \tag{7}$$

where $y = ((\rho_b I_B + 1)\varepsilon/\gamma_t)$, $\psi_m = M!/((M-m)!(m-1!))$, and $|\tilde{h}|^2 = |\hat{h}|^2 L(d)$ is the unordered channel gain of an arbitrary SU. Here, $\hat{h}$ is the small-scale fading coefficient with $\hat{h} \sim \mathcal{CN}(0,1)$, $L(d) = 1/(1+d^\alpha)$ is the large-scale path loss, and d is a random variable representing the distance from the secondary BS to an arbitrary SU.

Then, using the assumption of homogenous PPP and applying the polar coordinates, we express $F_{|\tilde{h}|^2}(y)$ as follows:

$$F_{|\tilde{h}|^2}(y) = \frac{2}{R_D^2} \int_0^{R_D} \left(1 - e^{-(1+r^\alpha)y}\right) r dr. \tag{8}$$

Note that it is challenging to obtain an insightful expression for the unordered cdf. As such, we apply the Gaussian–Chebyshev quadrature [13] to find an approximation for (8) as

$$F_{|\tilde{h}|^2}(y) \approx \sum_{n=0}^{N} b_n e^{-c_n y} \tag{9}$$

where N is a complexity–accuracy tradeoff parameter, $b_n = -\omega_N \sqrt{1-\phi_n^2}(\phi_n+1)$, $b_0 = -\sum_{n=1}^{N} b_n$, $c_n = 1 + ((R_D/2)(\phi_n+1))^\alpha$, $\omega_N = \pi/N$, and $\phi_n = \cos(((2n-1)/2N)\pi)$.

Substituting (9) into (7) and applying the multinomial theorem, we obtain

$$F_{|h_m|^2}(y) = \psi_m \sum_{p=0}^{M-m} \binom{M-m}{p} \frac{(-1)^p}{m+p} \times \sum_{\tilde{S}_m^p} \binom{m+p}{q_0+\cdots+q_N} \left(\prod_{n=0}^{N} b_n^{q_n}\right) e^{-\sum_{n=0}^{N} q_n c_n y} \tag{10}$$

where $\tilde{S}_m^p = \{(q_0, q_1, \ldots, q_K) | \sum_{i=0}^{K} q_i = m+p\}$, $\binom{m+p}{q_0+\cdots+q_N} = (m+p)!/q_0!, \ldots, q_N!$. Based on (10), the cdf of X_m can be expressed as follows:

$$\begin{aligned} F_{X_m}(\varepsilon_j) &= \int_0^\infty \int_0^\infty F_{|h_m|^2}\left(\frac{(\rho_b x + 1)\varepsilon_j}{z}\right) f_{I_B}(x) f_{\gamma_t}(z) dx dz \\ &= \psi_m \sum_{p=0}^{M-m} \binom{M-m}{p} \frac{(-1)^p}{m+p} \sum_{\tilde{S}_m^p} \binom{m+p}{q_0+\cdots+q_N} \\ &\quad \times \left(\prod_{n=0}^{N} b_n^{q_n}\right) \int_0^\infty e^{-\frac{\varepsilon_j}{z}\sum_{n=0}^{N} q_n c_n} Q_2 f_{\gamma_t}(z) dz \end{aligned} \tag{11}$$

where f_{γ_t} is the probability density function (pdf) of γ_t, and $Q_2 = \int_0^\infty e^{-(x\rho_b\varepsilon_j/z)\sum_{n=0}^{N} q_n c_n} f_{I_B}(x) dx$. We express Q_2 as follows:

$$Q_2 = E_{\Phi_b}\left\{e^{-\frac{x\rho_b\varepsilon_j}{z}\sum_{n=0}^{N} q_n c_n}\right\} = L_{I_B}\left(\frac{x\rho_b\varepsilon_j}{z}\sum_{n=0}^{N} q_n c_n\right). \tag{12}$$

In this case, the Laplace transformation of the interferences from the PT can be expressed as [10]

$$L_{I_B}(s) = \exp\left(-\lambda_b \pi \left[\left(e^{-s d_0^{-\alpha}} - 1\right) d_0^2 + s^\delta \underbrace{\int_0^{s d_0^{-\alpha}} t^{-\delta} e^{-t} dt}_{\Theta}\right]\right) \tag{13}$$

where $\delta = 2/\alpha$, and $\gamma(\cdot)$ is the lower incomplete Gamma function.

To obtain an insightful expression, we use the Gaussian–Chebyshev quadrature to approximate the lower incomplete Gamma function in (13), then Θ can be expressed as follows:

$$\Theta \approx s^{1-\delta} \sum_{l=1}^{L} \beta_l e^{-t_l s d_0^{-\alpha}} \tag{14}$$

where L is a complexity–accuracy tradeoff parameter, $\beta_l = (1/2) d_0^{2-\alpha} \omega_L \sqrt{1-\theta_l^2} t_l^{-\delta}$, $t_l = (1/2)(\theta_l + 1)$, $\omega_L = \pi/L$, and $\theta_l = \cos(((2l-1)/2L)\pi)$. Substituting (14) into (13), we approximate the Laplace transformation as follows:

$$L_{I_B}(s) \approx e^{-\lambda_b \pi \left(\left(e^{-s d_0^{-\alpha}} - 1\right) d_0^2 + s \sum_{l=1}^{L} \beta_l e^{-t_l s d_0^{-\alpha}}\right)}. \tag{15}$$

The following theorem provides the pdf of γ_t.

Theorem 1: Consider the use of the composite channel model with Rayleigh fading and path loss, the pdf of the effective power of the secondary BS is given by

$$\begin{aligned} f_{\gamma_t}(x) &= e^{-a_\ell \rho_s^\delta e^{-\frac{\rho_p}{x}}} \text{Dirac}(x - \rho_s) \\ &\quad + \left(\frac{\rho_p}{x} + \delta\right) a_\ell x^{\delta-1} e^{-a_\ell x^\delta e^{-\frac{\rho_p}{x}} - \frac{\rho_p}{x}} U(\rho_s - x) \end{aligned} \tag{16}$$

where $a_\ell = (\delta\pi\lambda_\ell\Gamma(\delta)/\rho_p^\delta)$, $U(\cdot)$ is the unit step function, and Dirac$(\cdot)$ is the impulse function.

Proof: See the Appendix. ∎

Substituting (15) and (16) into (11), using the Gaussian–Chebyshev quadrature similar as (14), we obtain the closed-form expression (17), shown at the bottom of the next page, of the outage probability at the mth user, where K is a complexity–accuracy tradeoff parameter, $\omega_K = \pi/K$, $\varphi_k = \cos(((2k-1)/2K)\pi)$, $s_k = (1/2)(\varphi_k + 1)$, and $\eta_k = (\omega_K/2)\sqrt{1-\varphi_k^2}((\rho_p/\rho_s s_k) + \delta(a_\ell \rho_s^\delta s_k^{\delta-1} e^{-a_\ell \rho_s^\delta s_k^\delta e^{-(\rho_p/\rho_s s_k)}}$.

IV. Diversity Analysis

Based on the analytical results for the outage probability in (17), we aim to provide an asymptotic diversity analysis for the ordered NOMA users. The diversity order of the user's outage probability is defined as

$$d = -\lim_{\rho_s \to \infty} \frac{\log P_m(\rho_s)}{\log \rho_s}. \tag{18}$$

A. Fixed Transmit Power at PTs

In this case, we examine the diversity with the fixed transmit SNR at the PTs (ρ_b), while the transmit SNR of the secondary BS (ρ_s) and the maximum permissible interference constraint at the PRs (ρ_p) go to the infinity. Particularly, we assume that ρ_p is proportional to ρ_s, i.e., $\rho_p = \kappa\rho_s$, where κ is a positive scaling factor. This assumption applies to

the scenario where the PRs can tolerate a large amount of interference from the secondary BS, and the target data rate is relatively small in the PN. Denote $\gamma_{t^*} = \gamma_t/\rho_s = \min\{\kappa/(\max_{\ell\in\Phi_\ell}|g_\ell|^2), 1\}$, similar to (7), the ordered cdf has the relationship with unordered cdf as

$$F^{\infty}_{X_m|I_B,\gamma_{t^*}}(y^*) = \psi_m \sum_{p=0}^{M-m} \binom{M-m}{p} \frac{(-1)^p}{m+p} \left(F^{\infty}_{|\tilde{h}|^2}(y^*)\right)^{m+p} \tag{19}$$

where $y^* = ((\rho_b I_B + 1)\varepsilon_j/\rho_s\gamma_{t^*})$. When $\rho_s \to \infty$, we observe that $y^* \to 0$. To investigate an insightful expression to obtain the diversity order, we use the Gaussian–Chebyshev quadrature and $1 - e^{-y^*} \approx y^*$ to approximate (8) as

$$F^{\infty}_{|\tilde{h}|^2}(y^*) \approx \sum_{n=1}^{N} \chi_n y^* \tag{20}$$

where $\chi_n = \omega_N\sqrt{1-\phi_n^2}(\phi_n+1)c_n$. Substituting (20) into (19), since $y^* \to 0$, we obtain

$$F^{\infty}_{X_m|I_B,\gamma_{t^*}}(\varepsilon_j) \approx \xi\left(\frac{(\rho_b I_B+1)\varepsilon_j}{\rho_s\gamma_{t^*}}\right)^m \tag{21}$$

where $\xi = (\psi_m(\sum_{n=1}^{N}\chi_n)^m)/m$. Based on (5), (10), and (21), the asymptotic outage probability is given by

$$P^{\infty}_{m_F} \approx \frac{1}{\rho_s^m} \times \underbrace{\int_0^{\infty}\int_0^{\infty} \xi\left(\frac{(\rho_b x+1)\varepsilon_{\max}}{z}\right)^m f_{I_B}(x) f_{\gamma_{t^*}}(z)\,dx\,dz}_{C} \tag{22}$$

where $f_{\gamma_{t^*}}$ is the pdf of γ_{t^*}. Since C is a constant independent of ρ_s, (22) can be expressed as follows:

$$P^{\infty}_{m_F} = \frac{1}{\rho_s^m} C + o\left({\rho_s}^{-m}\right). \tag{23}$$

Substituting (23) into (18), we obtain the diversity order of this case as m. This can be explained as follows. Note that SIC is applied at the ordered SUs. For the first user with the poorest channel gain, no interference cancelation is operated at the receiver; therefore, its diversity gain is 1. For the mth user, since the interferences from all the other $(m-1)$ users are canceled, it obtains a diversity of m.

B. Transmit Power of PTs Proportional to That of Secondary BSs

In this case, we examine the diversity with the transmit SNR at the PTs (ρ_b) proportional to the transmit SNR of the secondary BS (ρ_s). Particularly, we assume $\rho_b = \nu\rho_s$, where ν is a positive scaling factor. We still assume that ρ_p is proportional to ρ_s. Applying $\rho_s \to \infty$, $\rho_p = \kappa\rho_s$, and $\rho_b = \nu\rho_s$ to (17), we obtain the asymptotic outage probability of the mth user in this case as (24), shown at the bottom of the page, where $a_\ell^{\infty} = (\delta\pi\lambda_\ell\Gamma(\delta)/\kappa^\delta)$, and $\eta_k^{\infty} = (\omega_K/2)\sqrt{1-\varphi_k^2}((\kappa/s_k)+\delta)a_\ell^{\infty}s_k^{\delta-1}e^{-a_\ell^{\infty}s_k^{\delta}e^{-(\kappa/s_k)}}$.

It is observed that $P^{\infty}_{m_p}$ is a constant independent of ρ_s. Substituting (24) into (18), we find that, asymptotically, there is an error floor for the outage probability of SUs.

V. Numerical Results

Here, numerical results are presented to verify the accuracy of the analysis as well as to obtain more important insights for NOMA in

$$P_m = \psi_m \sum_{p=0}^{M-m} \binom{M-m}{p} \frac{(-1)^p}{m+p} \sum_{\tilde{S}_m^p} \binom{m+p}{q_0+\cdots+q_N} \left(\prod_{n=0}^{N} b_n^{q_n}\right) \times \left[e^{-a_\ell\rho_s^{\delta}e^{-\frac{\rho_p}{\rho_s}} - \frac{\varepsilon_{\max}\sum_{n=0}^{N} q_n c_n}{\rho_s} - \lambda_b\pi\left(\left(e^{-\frac{\rho_b\varepsilon_{\max}}{\rho_s d_0^{\alpha}}\sum_{n=0}^{N} q_n c_n} - 1\right) d_0^2 + \frac{\rho_b\varepsilon_{\max}}{\rho_s}\sum_{n=0}^{N} q_n c_n \sum_{l=1}^{L}\beta_l e^{-\frac{t_l\rho_b\varepsilon_{\max}}{\rho_s d_0^{\alpha}}\sum_{n=0}^{N} q_n c_n}\right)} + \sum_{k=1}^{K}\eta_k e^{-\frac{\rho_p+\varepsilon_{\max}\sum_{n=0}^{N} q_n c_n}{\rho_s s_k} - \lambda_b\pi\left(\left(e^{-\frac{\rho_b\varepsilon_{\max}}{\rho_s s_k d_0^{\alpha}}\sum_{n=0}^{N} q_n c_n} - 1\right) d_0^2 + \frac{\rho_b\varepsilon_{\max}}{\rho_s s_k}\sum_{n=0}^{N} q_n c_n \sum_{l=1}^{L}\beta_l e^{-\frac{t_l\rho_b\varepsilon_{\max}}{\rho_s s_k d_0^{\alpha}}\sum_{n=0}^{N} q_n c_n}\right)} \right] \tag{17}$$

$$P^{\infty}_{m_P} \approx \psi_m \sum_{p=0}^{M-m} \binom{M-m}{p} \frac{(-1)^p}{m+p} \sum_{\tilde{S}_m^p} \binom{m+p}{q_0+\cdots+q_N} \left(\prod_{n=0}^{N} b_n^{q_n}\right) \times \left[e^{-a_\ell^{\infty}e^{-\kappa} - \lambda_b\pi\left(\left(e^{-\frac{\nu\varepsilon_{\max}}{d_0^{\alpha}}\sum_{n=0}^{N} q_n c_n} - 1\right) d_0^2 + \nu\varepsilon_{\max}\sum_{n=0}^{N} q_n c_n \sum_{l=1}^{L}\beta_l e^{-\frac{t_l\nu\varepsilon_{\max}}{d_0^{\alpha}}\sum_{n=0}^{N} q_n c_n}\right)} + \sum_{k=1}^{K}\eta_k^{\infty} e^{-\frac{\kappa}{s_k} - \lambda_b\pi\left(\left(e^{-\frac{\nu\varepsilon_{\max}}{s_k d_0^{\alpha}}\sum_{n=0}^{N} q_n c_n} - 1\right) d_0^2 + \frac{\nu\varepsilon_{\max}}{s_k}\sum_{n=0}^{N} q_n c_n \sum_{l=1}^{L}\beta_l e^{-\frac{t_l\nu\varepsilon_{\max}}{s_k d_0^{\alpha}}\sum_{n=0}^{N} q_n c_n}\right)} \right] \tag{24}$$

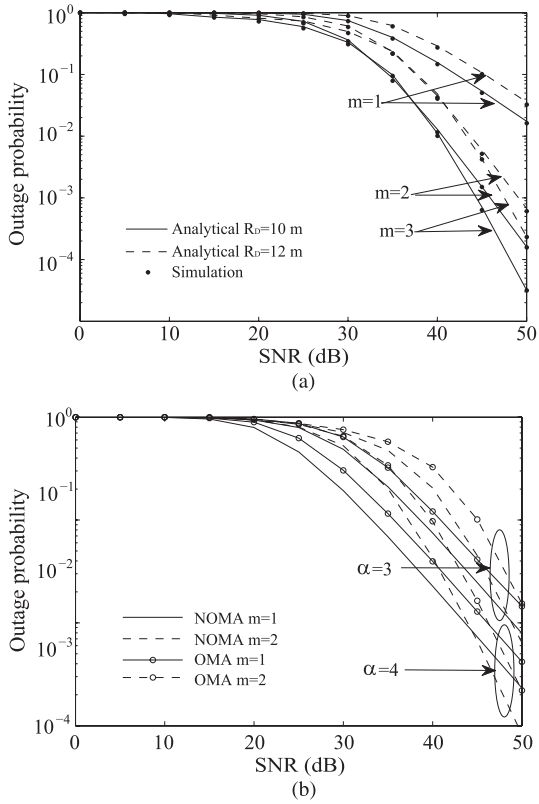

Fig. 1. Outage probability of the mth user versus ρ_s of the first scenario. (a) For different user zone, with $\lambda_b = 10^{-3}$, $\lambda_\ell = 10^{-3}$, $\kappa = 1$, $\alpha = 4$, $\rho_b =$ 20 dB, and $M = 3$. (b) For different α, with $\lambda_b = 10^{-3}$, $\lambda_\ell = 10^{-3}$, $\kappa = 1$, $R_D = 5$ m, $\rho_b = 20$ dB, and $M = 2$.

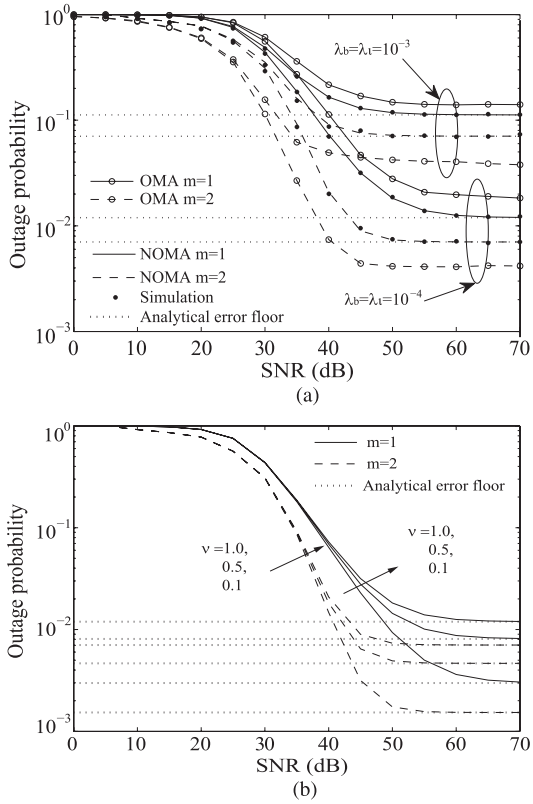

Fig. 2. Outage probability of the mth user versus ρ_s of the second scenario. (a) For different density of PTs and PRs, with $\alpha = 4$, $\kappa = 1$, $\nu = 1$, $R_D =$ 10 m, $\rho_b = \nu\rho_s$, and $M = 2$. (b) For different ν, with $\alpha = 4$, $\lambda_b = 10^4$, $\lambda_\ell = 10^4$, $\kappa = 0.5$, $R_D = 10$ m, $\rho_b = \nu\rho_s$, and $M = 2$.

large-scale CR networks. In the considered network, the radius of the guard zone is assumed to be $d_0 = 2$ m. The Gaussian–Chebyshev parameters are chosen with $N = 5$, $K = 10$, and $L = 10$. Monte Carlo simulation results are marked as "•" to verify our derivation.

Fig. 1 plots the outage probability of the mth user for the first scenario when ρ_b is fixed and ρ_p is proportional to ρ_s. In Fig. 1(a), the power allocation coefficients are $a_1 = 0.5$, $a_2 = 0.4$, and $a_3 = 0.1$. The target data rate for each user is assumed to be the same as $R_1 = R_2 = R_3 = 0.1$ bits per channel use (BPCU). The dashed and solid curves are obtained from the analytical results derived in (17). Several observations can be drawn as follows: 1) Reducing the coverage of the SUs zone $\mathcal{D}$ can achieve a lower outage probability because of a smaller path loss; 2) the ordered users with different channel conditions have different decreasing slopes because of different diversity orders, which verifies the derivation of (22). In Fig. 1(b), the power allocation coefficients are $a_1 = 0.8$ and $a_2 = 0.2$. The target rate is $R_1 = 1$ and $R_2 = 3$ BPCU. The performance of a conventional OMA is also shown in the figure as a benchmark for comparison. It can be observed that for different values of the path loss, NOMA can achieve a lower outage probability than the conventional OMA.

Fig. 2 plots the outage probability of the mth user for the second scenario when both ρ_b and ρ_p are proportional to ρ_s. The power allocation coefficients are $a_1 = 0.8$ and $a_2 = 0.2$. The target rates are $R_1 = R_2 = 0.1$ BPCU. The dashed and solid curves are obtained from the analytical results derived in (17). One observation is that error floors exist in both Fig. 2(a) and (b), which verifies the asymptotic results in (24). Another observation is that user 2 $(m = 2)$ outperforms user 1 $(m = 1)$. The reason is that for user 2, by applying SIC, the interference from user 1 is canceled. On the other hand, for user 1, the interference from user 2 still exists. In Fig. 2(a), it is shown that the error floor becomes smaller when λ_b and λ_ℓ decrease, which is due to less interference from PTs and the relaxed interference power constraint at the PRs. It is also worth noting that with these system parameters, NOMA outperforms OMA for user 1, whereas OMA outperforms NOMA for user 2, which indicates the importance of selecting appropriate power allocation coefficients and target data rates for NOMA. In Fig. 2(b), it is observed that the error floors become smaller as ν decreases. This is due to the fact that smaller ν means lower transmit power of PTs, which, in turn, reduces the interference at SUs.

VI. Conclusion

In this paper, we have studied NOMA in large-scale underlay CR networks with randomly deployed users. Stochastic geometry tools were used to evaluate the outage performance of the considered network. New closed-form expressions were derived for the outage probability. Diversity order of NOMA users has been analyzed in two situations based on the derived outage probability. An important future direction is to optimize the power allocation coefficients to further improve the performance gap between NOMA and conventional MA in CR networks.

Appendix
Proof of Theorem 1

The cdf of γ_t is given as

$$F_{\gamma_t}(x) = 1 - U(\rho_s - x) \underbrace{\Pr\left\{\max_{\ell\in\Phi_\ell} |g_\ell|^2 \geq \frac{\rho_p}{x}\right\}}_{\Omega}. \tag{A.1}$$

Denote $\bar{\Omega} = 1 - \Omega$, we express $\bar{\Omega}$ as follows:

$$\bar{\Omega} = E_{\Phi_\ell}\left\{\prod_{\ell\in\Phi_\ell} F_{|\hat{g}_\ell|^2}\left(\frac{\left(1+d_\ell^\alpha\right)\rho_p}{x}\right)\right\}. \tag{A.2}$$

Applying the generating function, we rewrite (A.2) as follows:

$$\begin{aligned}\bar{\Omega} &= \exp\left[-\lambda_\ell \int_{R^2}\left(1 - F_{|\hat{g}_\ell|^2}\left(\left(1+d_\ell^\alpha\right)\mu\right)\right) r dr\right] \\ &= \exp\left[-2\pi\lambda_\ell e^{-\mu}\int_0^\infty r e^{-\mu r^\alpha} dr\right]. \end{aligned}\tag{A.3}$$

Applying [14, eq. (3.326.2)], we obtain

$$\Omega = 1 - \bar{\Omega} = 1 - e^{-\frac{e^{-\mu}\delta\pi\lambda_\ell\Gamma(\delta)}{\mu^\delta}} \tag{A.4}$$

where $\Gamma(\cdot)$ is the Gamma function. Substituting (A.4) into (A.1) and taking the derivative, we obtain the pdf of γ_t in (16). The proof is completed.

REFERENCES

[1] Y. Saito, A. Benjebbour, Y. Kishiyama, and T. Nakamura, "System-level performance evaluation of downlink non-orthogonal multiple access (NOMA)," in *Proc. IEEE Annu. Symp. PIMRC*, Sep. 2013, pp. 611–615.

[2] Z. Ding, Z. Yang, P. Fan, and H. V. Poor, "On the performance of non-orthogonal multiple access in 5G systems with randomly deployed users," *IEEE Signal Process. Lett.*, vol. 21, no. 12, pp. 1501–1505, Dec. 2014.

[3] M. Al-Imari, P. Xiao, M. A. Imran, and R. Tafazolli, "Uplink non-orthogonal multiple access for 5G wireless networks," in *Proc. IEEE 11th ISWCS*, Barcelona, Spain, Aug. 2014, pp. 781–785.

[4] Z. Ding, F. Adachi, and H. V. Poor, "The application of MIMO to non-orthogonal multiple access," *IEEE Trans. Wireless Commun.*, vol. 15, no. 1, pp. 537–552, Jan. 2016.

[5] Q. Sun, S. Han, C.-L. I, and Z. Pan, "On the ergodic capacity of MIMO NOMA systems," *IEEE Wireless Commun. Lett.*, vol. 4, no. 4, pp. 405–408, Aug. 2015.

[6] A. Goldsmith, S. A. Jafar, I. Maric, and S. Srinivasa, "Breaking spectrum gridlock with cognitive radios: An information theoretic perspective," *Proc. IEEE*, vol. 97, no. 5, pp. 894–914, May 2009.

[7] Y. Dhungana and C. Tellambura, "Outage probability of underlay cognitive relay networks with spatially random nodes," in *Proc. GLOBECOM*, Dec. 2014, pp. 3597–3602.

[8] Z. Ding, P. Fan, and H. V. Poor, "Impact of user pairing on 5G non-orthogonal multiple access," *IEEE Trans. Veh. Technol.*, vol. 65, no. 8, pp. 6010–6023, Aug. 2016.

[9] M. Haenggi, *Stochastic Geometry for Wireless Networks*. Cambridge, U.K.: Cambridge Univ. Press, 2012.

[10] J. Venkataraman, M. Haenggi, and O. Collins, "Shot noise models for outage and throughput analyses in wireless ad hoc networks," in *Proc. MILCOM*, 2006, pp. 1–7.

[11] T. M. Cover and J. A. Thomas, *Elements of Information Theory*, 2nd ed. New York, NY, USA: Wiley, 2006.

[12] H. A. David and N. Nagaraja, *Order Statistics*, 3rd ed. New York, NY, USA: Wiley, 2003.

[13] E. Hildebrand, *Introduction to Numerical Analysis*. New York, NY, USA: Dover, 1987.

[14] I. S. Gradshteyn and I. M. Ryzhik, *Table of Integrals, Series and Products*, 6th ed. New York, NY, USA: Academic, 2000.

A Differential ML Combiner for Differential Amplify-and-Forward System in Time-Selective Fading Channels

Yi Lou, Yong-Kui Ma, Qi-Yue Yu, *Member, IEEE*, Hong-Lin Zhao, *Member, IEEE*, and Wei Xiang, *Senior Member, IEEE*

***Abstract*—We propose a new differential maximum-likelihood (DML) combiner for noncoherent detection of the differential amplify-and-forward (D-AF) relaying system in the time-selective channel. The weights are computed based on both the average channel quality and the correlation coefficient of the direct and relay channels. Moreover, we derive a closed-form approximate expression for the average bit error rate (BER), which is applicable to any single-relay D-AF system with fixed weights. Both theoretical and simulated results are presented to show that the time-selective nature of the underlying channels tends to reduce the diversity gains at the low-signal-to-noise-ratio (SNR) region, resulting in an asymptotic BER floor at the high-SNR region. Moreover, the proposed DML combiner is capable of providing significant BER improvements compared with the conventional differential detection (CDD) and selection-combining (SC) schemes.**

***Index Terms*—Amplify and forward (AF), differential modulation, noncoherent detection, performance analysis, time-varying channels.**

I. INTRODUCTION

Cooperative communications has received much attention since it is capable of improving system performance and extending coverage. Thus, several relay-assisted architectures have been adopted by the Third Generation Partnership Project Long Term Evolution-Advanced and IEEE 802.16j standards [1]. It is widely anticipated that cooperative communications will act as a key technology for fifth-generation [2]–[4] mobile communications. Amplify and forward (AF) [5] is a viable technique of cooperative communications from the practical point of view because of its simple implementation and security [6].

It is well known that a moving terminal will induce the Doppler shift, which is the cause of the time selectivity in the fast-fading channel. The impact of outdated channel state information (CSI) on the AF relaying system that employs a relay selection scheme is analyzed in [7] and [8]. The same impact analysis is then extended to the turbo coded relay system over the Nakagami-m channel in [9]. In [10], a weighted two-way relay-selection scheme was proposed whereby the weights take into consideration the correlation coefficient of the time-selective channel. In [11], the impact of different CSI estimation rates on the error performance of a multirelay AF system employing maximal ratio that combines over the time-selective fading channel was studied. Then, the same performance analysis was extended to relay selection in the presence of channel estimation errors in [12].

Manuscript received August 17, 2015; revised December 16, 2015; accepted February 21, 2016. Date of publication February 26, 2016; date of current version December 14, 2016. This work was supported in part by the Key Laboratory of Universal Wireless Communications (Beijing University of Posts and Telecommunications), Ministry of Education of China. The review of this paper was coordinated by Prof. J. P. Coon.

Y. Lou, Y.-K. Ma, Q.-Y. Yu, and H.-L. Zhao are with the Department of Communication Engineering, Harbin Institute of Technology, Harbin 150001, China (e-mail: louyi8733@gmail.com; yk_ma@hit.edu.cn; yuqiyue@hit.edu.cn; hitbourne@gmail.com).

W. Xiang is with the College of Science, Technology and Engineering, James Cook University, Cairns, Qld. 4870, Australia (e-mail: wei.xiang@jcu.edu.au).

Color versions of one or more of the figures in this paper are available online at http://ieeexplore.ieee.org.

Digital Object Identifier 10.1109/TVT.2016.2535299